Investigation of magnetic and optical properties on dopant concentration of Ni based $BaTiO_3$ ceramics

R. Rajalakshmi [a, b], T. Thangeeswari [c], S. Senthil [d], R. Kavitha [e], V. Ratchagar [f], S. Chandra [a, g, *]

[a] *Department of Physics, Annamalai University, Chidambaram-608 002, Tamilnadu, India*

[b] *Department of Physics, CK College of Engineering and Technology, Cuddalore, Tamil Nadu 607003, India*

[c] *Department of Physics, Vel Tech Multitech Dr. Rangarajam Dr. Sakunthala Engineering College, Chennai-600 062, Tamilnadu, India*

[d] *Department of Physics, Chennai Institute of Technology, Chennai-600069, Tamilnadu, India*

[e] *Department of Physics, Rajalakshmi Institute of Technology, chennai-600 124, Tamilnadu, India*

[f] *Department of Physics, IFET College of Engineering (Autonomous), Villupuram-605 108, Tamilnadu, India*

[g] *Department of Physics, Govt. Arts College for Women, Salem-636 008, Tamilnadu, India*

Pure barium titanate (BTO) perovskite ceramics, 1% and 3% nickel (Ni) doped BTO ceramics were synthesized by solid-state reaction method. Structural, morphological, optical, and magnetic characteristics were analyzed by X-ray powder diffraction (XRD), Fourier infrared spectroscopy (FTIR), scanning electron microscopy, energy dispersive X-ray analysis (EDAX), UV-vis-spectrophotometer (UV), and vibrating sample magnetometer (VSM.) In XRD patterns by using Scherrer formula the crystalline size of BTO perovskite ceramics, 1% and 3% Ni-doped BTO ceramics was determined as 7.87 nm, 4.67 nm and 15.54 nm. The volume of unit cell was reduced in 1% and 3% nickel doped BTO. The estimated c/a ratio for all three synthesized samples BTO, 1% and 3% Ni-doped BTO ceramics substantiates that the symmetry of the synthesized samples remains unmodified. FTIR spectra revealed the existence of functional groups. SEM images confirmed the dopant of Ni in $BaTiO_3$ ceramics does not produce any changes in the morphology even at high concentrations of doping. EDAX spectra implied that the atomic concentration of elements presents in pure BTO, 1% and 3% Ni-doped BTO ceramics.

(Received April 28, 2025; Accepted August 13, 2025)

Keywords: Perovskite structure, Barium titanate, Magnetic properties, Bandgap value, Ceramics

1. Introduction

Barium titanate is an excellent ferro electric ceramic material with unique properties such as positive temperature coefficient, optoelectronics, enhanced dielectric permittivity, pyro and piezoelectric characteristics [1]. Barium titanate ($BaTiO_3$) has a tetragonal perovskite structure with the typical formula ABO_3. The A site (Ba^{2+}) and B (Ti^{4+}) are the two distinct metal cations with varying sizes. Both metal cations are bonded with oxygen anions. In general, size of the A site in perovskite structure is greater than the B site [2]. Due to its numerous unique properties, BaTiO3 is used in various technical applications, such as capacitors, to store data, transducers, and sensors to detect pollutants like carbon monoxide [3].

* Corresponding author: shanmugamchandra81@gmail.com
https://doi.org/10.15251/DJNB.2025.203.957

Recent research work moves towards the industrial needs for enhanced performance of all electronic devices by doping various metals with $BaTiO_3$. Many research results confirm that the doping of various metals with $BaTiO_3$ lattice increases their ferro, pyro, and piezoelectric properties. Baiju et al. observed that the doping of cobalt ions with $BaTiO_3$ shows a greater dielectric constant than pure $BaTiO_3$. This arises due to the process of distortion in the lattice and crystallized size [3, 4]. Chen et al. noticed that the inclusion of nickel in the $BaTiO_3$ lattice drastically enriches the dielectric constant. Further increases the doping concentration of nickel with $BaTiO_3$ making the sample as conducting material [5]. Kundu et al. research confirmed that the dielectric behavior influenced by the concentration of metal inclusions in $BaTiO_3$ [6]. On data storage devices, we need reading and writing to be done simultaneously. Further, we need materials with both ferroelectric and ferromagnetic properties called magneto-electric materials, which make the data written electrically and read magnetically. Revathy et al. observed that nickel doped $BaTiO_3$ possesses magneto-electric properties, which make it a promising material for magnetic memory devices [7].

The present research work describes the synthesis of pure BaTiO3 (BTO) ceramics and 1 and 3% nickel-doped BTO ceramics via the solid-state reaction method. From synthesized samples with various characterization techniques, we reported the effect of doping on tuning the physical, magnetic, and optical properties of BaTiO3 ceramics.

2. Experimental performance

2.1. Material synthesis

Nickel-doped $BaTiO_3$ samples were synthesized by the solid-state reaction method. It is the process of mechano-chemical reaction that takes place in solid-state powders without any solvent usage. The advantage of this method is that it is low-cost, pollution-free, simple to process, and gives samples on a large scale [8]. As starting materials, extremely pure powders of analytical reagent (AR) grade $BaCo_3$ (>99.5%), TiO_2 (>99.9%), and Ni (>99.0%) were used. Weighings of undoped and Ni-doped barium titanate (BTO) were performed using the stoichiometric composition (x=1% and 3%) using a solid-state method. After being heated to 100° C for an hour on a hot plate, the weighed raw powders were fully combined in an agitated mortar with acetone acting as a solvent for an additional hour. After that, the samples were dried for three hours at 400° in a furnace. To achieve high crystallinity, the samples were once more crushed for 15 minutes and then calcified for 8 hours at 900°C. Lastly, numeral characterizations were performed on the produced samples.

2.2. Characterization methods

By utilising Cu Kα radiation (λ=1.5406Å) and a examine rate of $0.05°s^{-1}$, pure $BaTiO_3$ (BTO) ceramics, 1% and 3% nickel-doped BTO ceramics were examined using X-ray diffraction in the 2θ range from 0° to 90° (BRUKER USA D8 Advance, Davinci). Morphological analysis was done by Scanning Electron Microscopy (SEM, Hitachi S-3000N, Tokyo, Japan, 0.3 - 30kV). The functional groups were identified by FTIR spectra with PERKIN ELMER Infrared spectrophotometer to investigate the optical characteristics of the produced ceramics, a Shimadzu UV-2450 UV-Vis spectrophotometer was used.

3. Results and discussions

3.1. Phase analysis from XRD patterns

X-ray diffraction analysis helps to find the doping effect on the host sample by analyzing the diffraction peaks. The X-ray diffraction patterns of BTO, 1%, and 3% Ni-doped BTO are shown in figure 1. XRD analysis confirms the tetragonal phases of all three synthesized samples. When Ni ion is doped with BTO ceramics, the diffraction peaks are slightly shifted to the right. The diffraction peaks broaden with high intensity for heavily doped 3% Ni compared to 1% Ni. In high concentration 3% Ni-doped BTO, the additional peaks with split-up are observed at 41.27°,

46°, and 31.39° [9]. This change in the peaks clearly confirmed that the dopant Ni ion is successfully incorporated into the BTO lattice site [10]. The ionic radius of the Ni $^{2+}$ ion is 0.72 and that of the Ti $^{4+}$ ion is 0.605, which is an approximately very close value. Further, there is the possibility of the Ni^{2+} ion replacing the Ti^{4+} ion in the B site. This substitution of the Ni $^{2+}$ ion created oxygen vacancies in the lattice site. The crystalline size was found by applying the Scherrer's formula.

$$D = 0.89\lambda/\beta \cos\theta$$

where D is the size of the particle, is the incident X-ray wavelength (1.5406 A°), is the full width half maxima (FWHM), and θ is the Bragg diffraction angle. The crystalline sizes of pure BTO, 1%, and 3% Ni-doped BTO ceramics were found to be in the range of 7.87 nm, 4.67 nm, and 15.54 nm, respectively. The high concentration of Ni-doped samples showed a larger crystalline size, which confirms the presence of Ni^{2+} in the BTO ceramic lattice. The lattice parameter (a) was increased with an increase in nickel ions concentration. The c/a ratio for all three synthesized samples (BTO, 1%, and 3% Ni-doped BTO) was in the range of 1, which confirms that the symmetry of the synthesized samples remains unchanged. This result authenticates that the doping element and its concentration are a good choice [11]. The unit cell volume of nickel 1% and 3% doped BTO was found to decrease from 65.40 A° (pure) to 64.4874 A° (3% Ni). This reduction in cell volume proves the perfect replacement of Ti^{4+} ions by the doped ion Ni^{2+} in the BTO ceramic lattice, which is concurred with XRD results. The computed values of crystallite size, lattice parameters, and volume of unit cell are reported in Table 1.

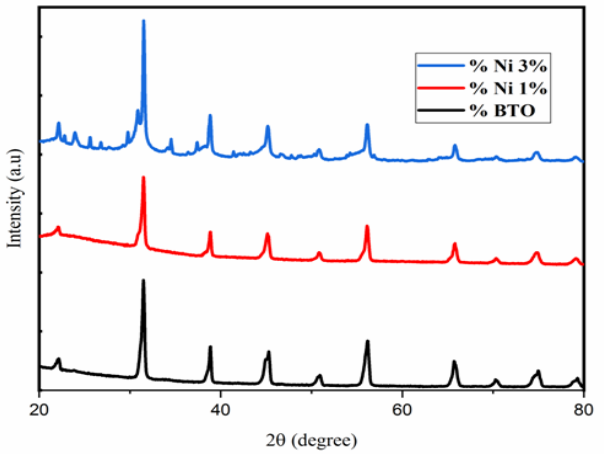

Fig. 1. XRD patterns of BTO, 1% and 3% Ni doped BTO ceramics.

Table 1. Micro structural property of pure BTO, 1% and 3% Ni doped BTO ceramics.

Sample	Average particle size (nm)	a (A°)	c(A°)	c/a Ratio	Unit cell volume (A°)
BTO	7.87	4.00415	4.07931	1.019	65.4045
BTO/Ni 1%	4.67	4.00665	4.01497	1.002	64.4502
BTO/Ni 3%	15.54	4.01489	4.01485	1.000	64.4874

3.2. Functional group analysis by FTIR spectroscopy

FTIR spectroscopic examination depicts the existence of functional groups. FTIR spectrum in figure 2 gives the information about oxide formation in synthesized samples of BTO, 1% and 3% Ni doped BTO ceramics. The peaks around 1450 cm^{-1} in all samples, such as BTO, 1% and 3% Ni doped BTO correspond to the Ba-Ti-O stretching bond, which authenticates the

existence of barium titanate in all three synthesized samples [3]. The characteristic peaks at 776 cm^{-1} and 772 cm^{-1} are observed for BTO and 1% Ni doped BTO ceramics. This peak is attributed to the presence of a carbonyl group, which is not found in higher concentrations of nickel (3% Ni) doped sample [12]. BTO, 1% and 3% Ni doped BTO ceramics show peaks near 500 cm^{-1} which correspond to Ti-O and Ti-O-Ti bonds [13].

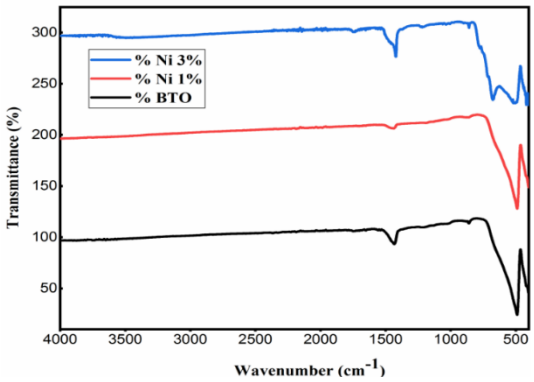

Fig. 2. FTIR Spectra of BTO, 1% and 3% Ni doped BTO ceramics.

3.3. Morphological study

In figure 3, FESEM results give the morphology of pure BTO, 1% and 3% Ni-doped BTO ceramics. Agglomeration of particles with irregular cluster form was observed in the high concentration doped sample of 3% Ni- BTO compared to 1% Ni-BTO. But in pure BTO ceramics, we observed distinct particles with very little agglomeration [14, 15]. From the SEM results, it was noticed that the process of doping does not affect the morphology even at high concentrations but only varies the crystalline size, which is matched with above XRD results.

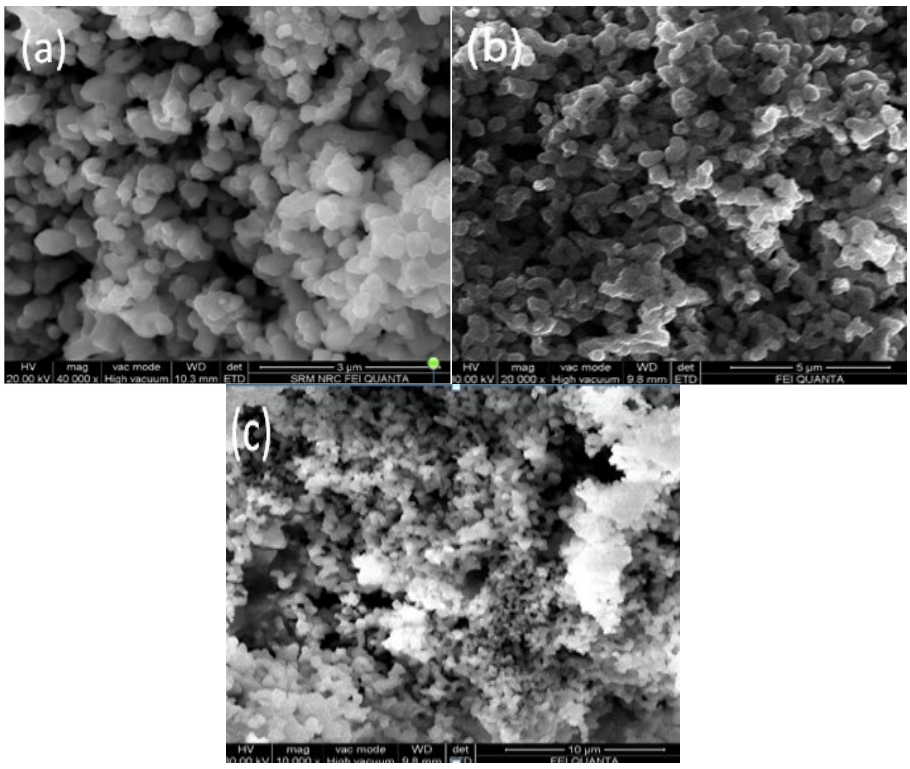

Fig. 3. SEM Images of a) Pure BTO, b) 1% Ni doped BTO Ceramics c) 3% Ni doped BTO ceramics.

Figure 4 (a–c) depicts the EDAX spectrum of pure BTO, 1%, and 3% Ni doped BTO ceramics. EDAX analysis is used to confirm the composition of the elements present in the synthesized samples.The atomic concentrations of elements present in pure BTO, 1%, and 3% Ni-doped BTO ceramics are revealed in Table 2. This spectrum confirms the presence of the elements Ti, Ba, Ni, and O in our synthesized samples.

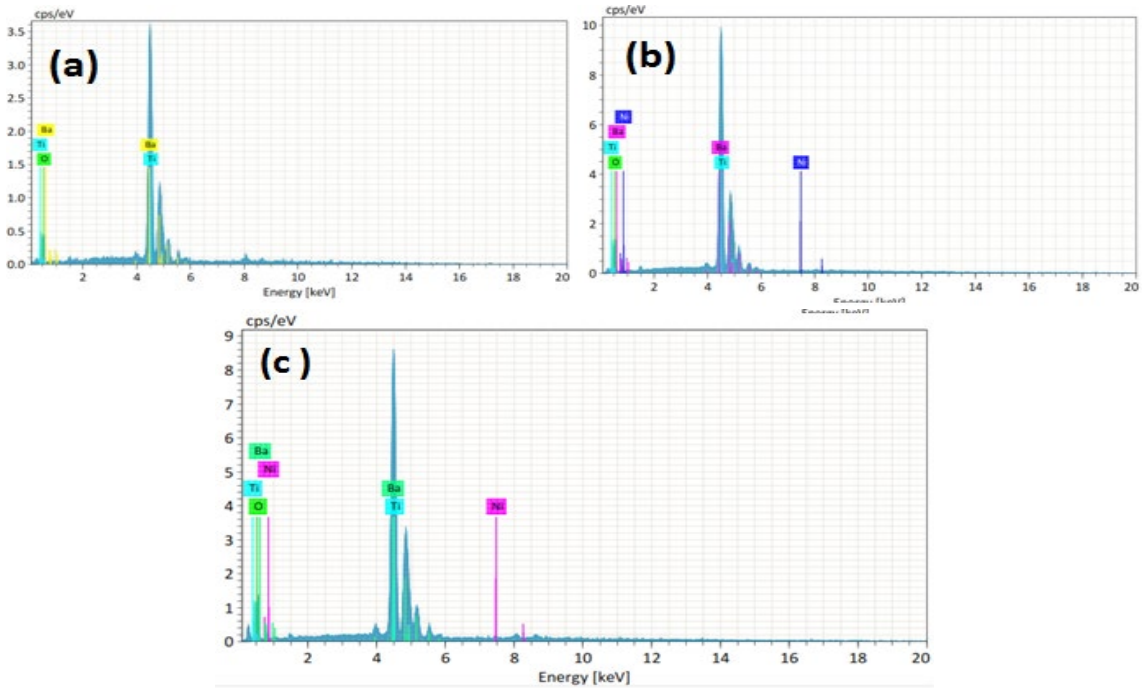

Fig. 4. EDAX Spectra of a) Pure BTO, b) 1% Ni doped BTO Ceramics c) 3% Ni doped BTO ceramics.

Table 2. Atomic concentration of elements presents in pure BTO, 1% and 3% Ni doped BTO Ceramics from the EDAX analysis.

Particle Name	**Atomic % of Ba**	**Atomic % of Ti**	**Atomic % of O**	**Atomic % of Ni**
BTO	18	35.84	46.04	---
BTO/Ni 1%	19.14	36.53	44.02	0.30
BTO/Ni 3%	24.35	30.43	44.61	0.61

3.4. Optical studies

Figure 5 illustrates the UV-visible absorption spectra of pure BTO, 1% and 3% Ni-doped BTO perovskite ceramics. The spectra show the absorption peaks at 388 nm, with one maximum peak approximately at 282 nm [16]. Mukherjee et al. results confirm that the shift of the absorption band corresponds to a change in the lattice parameter of the BTO perovskite structure, which arises due to the incorporation of nickel ions in place of Ti^{4+}ions [14]. Further, it is observed that there is a red shift in absorbance for 3% Ni-doped BTO perovskite ceramics compared to pure BTO and 1% Ni-doped BTO perovskite ceramics [3]. The absorption peak at 388 for all three samples of pure BTO, 1%, and 3% Ni-doped BTO perovskite ceramics may arise due to band-to-band changeover in BTO perovskite ceramics [17].

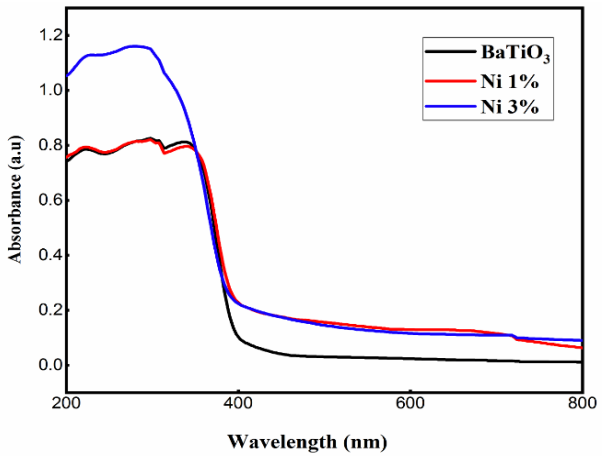

Fig. 5. UV Absorption spectra of a) Pure BTO, b) 1% Ni doped BTO Ceramics c) 3% Ni doped BTO ceramics.

Optical bandgap (Eg) is the parameter that changes the optical and magnetic properties of pure BTO, 1% and 3% Ni-doped BTO perovskite ceramics. Optical bandgap was estimated by using the Tauc method, which gives a relation between absorption coefficient (α) and photon energy (hυ). To get the bandgap value, the graph is drawn between (αhν)2 and photon energy hν, and the linear extrapolation of the drawn curve is done. From figure 6, it was estimated that the optical band gap values of pure BTO, 1% and 3% Ni-doped BTO perovskite ceramics are 3.20, 3.13, and 3.10 eV, respectively. It is confirmed that the nickel-doped BTO perovskite ceramics show a reduction in bandgap values. This reduction in bandgap may correspond to the formation of new energy bands due to the inclusion of nickel into the BTO perovskite ceramic lattice [17].

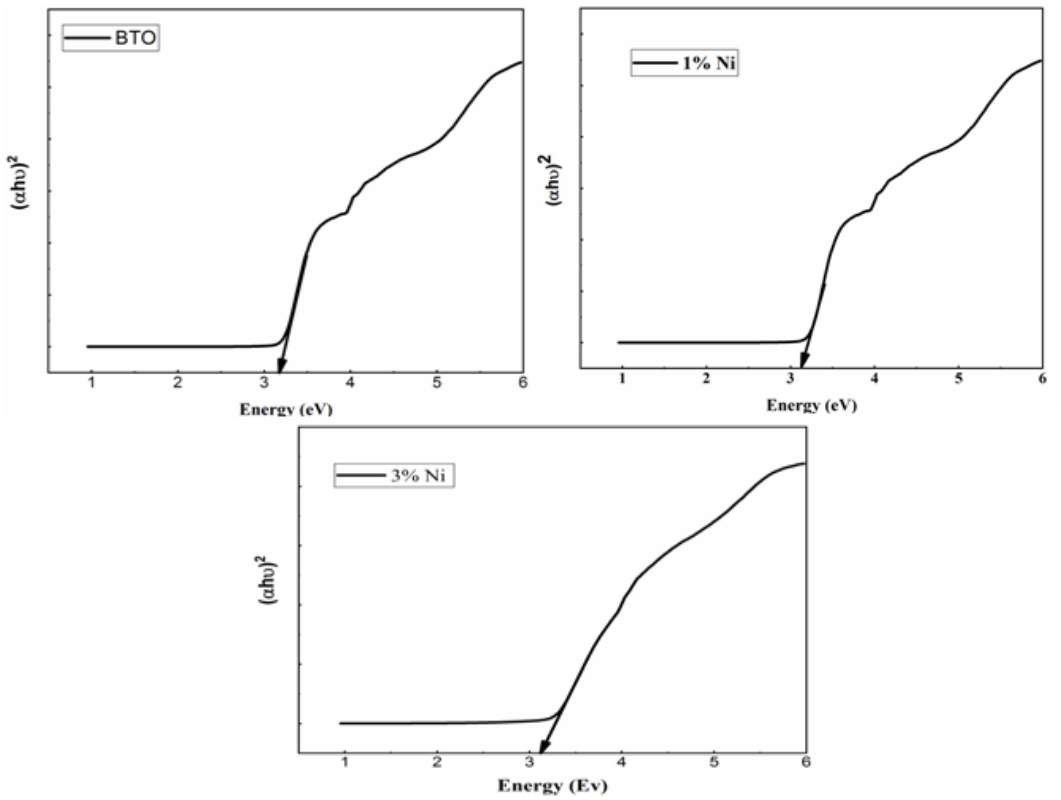

Fig. 6. Bandgap Spectra of a) Pure BTO, b) 1% Ni doped BTO Ceramics c) 3% Ni doped BTO ceramics.

3.5. Magnetic studies

The M-H curves in figure 7 give the detailed magnetic properties of pure BTO, 1% and 3% Ni-doped BTO ceramics. The value of magnetization is enhanced for 1% of Ni doped BTO ceramics and then decreased for 3% of Ni-doped BTO ceramics. Enhancement of magnetization in 1% of Ni-doped BTO ceramics may be attributed to a reduction in its bandgap value [18]. An increase in magnetization arises from the increase in charge carrier concentration due to interparticle interactions. Pure BTO shows diamagnetic characteristics, which are the intrinsic nature of BTO ceramics [9]. For 1% and 3% Ni-doped BTO ceramics, the spectra reveal their paramagnetic nature. This paramagnetic behavior arises from the addition of nickel ions in the tetragonal phases of BTO ceramics [19]. On the other side, the absence of a ferromagnetic hysteresis curve confirms the absence of secondary phases, which is in concordance with our XRD results [20]. Liu et al.'s results prove that the dopant cobalt alone is not the responsible factor for the magnetic properties of cobalt in $BaTiO_3$, which also contributes to defects due to oxygen vacancy [21]. Coercivity value of 1% nickel-doped $BaTiO_3$ ceramics decreases when compared to 3% nickel-doped $BaTiO_3$ ceramics and pure $BaTiO_3$ ceramics. This reduction in coercivity value confirms the well-built interparticle exchanges that take place in 1% nickel-doped $BaTiO_3$ ceramics compared to 3% nickel-doped $BaTiO_3$ ceramics and pure $BaTiO_3$ ceramics [22].

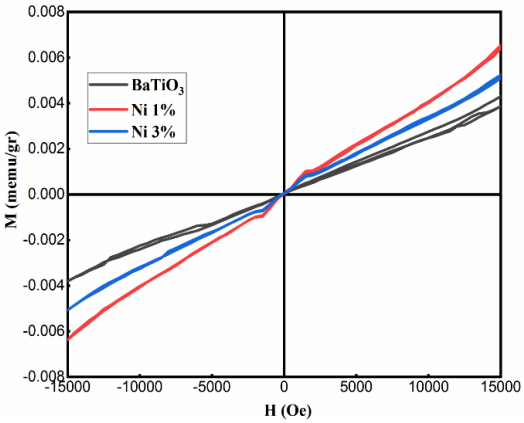

Fig. 7. M-H curves ofa) Pure BTO, b) 1% Ni doped BTO Ceramics c) 3% Ni doped BTO Ceramics.

4. Conclusion

In this study, we investigated the structural, morphological, optical, and magnetic properties of the pure BTO, 1%, and 3% Ni-doped BTO perovskite ceramic samples produced by the solid-state reaction method. Lattice parameter increases with an increase in dopant nickel concentration. Particle size decreases with 1% nickel doping and again increases with 3% nickel concentration. The reduction in unit cell volume observed in 1% and 3% Ni-doped BTO perovskite ceramics authenticates the perfect replacement of Ti4+ ions by the doped ion Ni2+ in the BTO ceramic lattice. FTIR results confirm that all three synthesized samples have BTO perovskite ceramic structures. Further, optical studies revealed that the bandgap value is condensed from 3.20 eV to 3.10 eV for nickel dopant BTO ceramics. Moreover, the reduction in bandgap was due to the formation of new energy bands in the BTO perovskite ceramic lattice when nickel is included. Nickel-doped tetragonal-phase BTO perovskite ceramics show the paramagnetic property at room temperature. This paramagnetic characteristic may arise due to oxygen vacancy, and the decrease in coercivity value for nickel-doped tetragonal phase BTO perovskite ceramics confirms the inter-particle interactions.

References

[1] Suravi Islam, NaziaKhatun, Md. Shehan Habib, Syed Farid Uddin Farhad, Nazmul Islam

Tanvir, Heliyon, 8 (2022) 10529; https://doi.org/10.1016/j.heliyon.2022.e10529

[2] MahasenReda,S. I. El-Dek, M. M. Arman, J Mater Sci Mater Electron 33 2022, 16753-16776; https://doi.org/10.1007/s10854-022-08541-x

[3] Kuttappan Gireesh Baiju, Aishwarya Nagarajan, Akshaya Marappa Gounder Sadasivam, Deva Darsan Sukumar Rajan, Karlapudi Sri Sai Vignathi, Murali Balu, Duraisamy Kumaresan, J ChemEngg, 2550, 2020, 1-9.

[4] Masatomo Yashima, Takuya Hoshina, Daiju Ishimura, Syuuhei Kobayashi, Wataru Nakamura, J Applied Phys, 98, 014313, 2005; https://doi.org/10.1063/1.1935132

[5] Renzheng Chen, Xiaohui Wang, Hai Wen, Longtu Li, ZhilunGui, Ceramics International 30 (2004) 1271-1274; https://doi.org/10.1016/j.ceramint.2003.12.049

[6] T K Kundu, A Jana, P. Barick, Bull Mater Sci, 31, 2008, 501-505; https://doi.org/10.1007/s12034-008-0078-1

[7] Ramany Revathy, Aswathi Kaipamangalath, Manoj Raama Varma, Kuzhichalil Peethambharan Surendran, New J Chem., 44 2020 3690-3699; https://doi.org/10.1039/C9NJ05532K

[8] Ruxangul Jamal, Feng Xu, Weiwei Shao, Tursun Abdiryim, Nanoscale Research Lett, 8, 2013, 1-8; https://doi.org/10.1186/1556-276X-8-117

[9] S.K. Das, R.N. Mishra, B.K. Roul, Solid State Communications 191 (2014) 19-24; https://doi.org/10.1016/j.ssc.2014.04.001

[10] Kazuhiko Maeda, ACS Appl. Mater. Interfaces 2014, 6, 2167−2173; https://doi.org/10.1021/am405293e

[11] Mahasen Reda, S. I. El-Dek, M. M. Arman, J Mater Sci: Mater Electron (2022) 33:16753-16776; https://doi.org/10.1007/s10854-022-08541-x

[12] Anuradha Kumari, Barnali Dasgupta Ghosh, A study of dielectric behavior of manganese doped barium titanate-polyimide composites, Wiley, 2017; https://doi.org/10.1002/adv.21886

[13] Mohammed Tihtih, Karoum Limame, Yahya Ababou, Salaheddine Sayouri, Jamaleldin F. M. Ibrahim, Journal of Silicate Based and Composite Materials, 71 (6), 190-193, 2019; https://doi.org/10.14382/epitoanyag-jsbcm.2019.33

[14] Pedro E. Sánchez-Jiménez, Luis A. Pérez-Maqueda, María J. Diánez, Composite Structures 92 (2010) 2236-2240; https://doi.org/10.1016/j.compstruct.2009.08.011

[15] Soumya Mukherjee, S. Ghosh, C. Ghosh, J. Inst. Eng. India Ser. D , 2013 94(1), 57-64; https://doi.org/10.1007/s40033-013-0019-z

[16] Adil Alshoaibi, Osama Saber, and Faheem Ahmed, Crystals 2021, 11, 550; https://doi.org/10.3390/cryst11050550

[17] Maerin Cernia. Mihail Secu, Roxana Radu, Paul Ganeaa, Vasile Adrian Surdub, Roxana Truscab, Eugenia Tanasa Vasile, Elisabeta Corina Secu, Journal of Alloys and Compounds 878 (2021) 160380; https://doi.org/10.1016/j.jallcom.2021.160380

[18] Ying Zhang, S. Das Sarma, Phys. Rev. B 72, 125303 (2005); https://doi.org/10.1103/PhysRevB.72.125303

[19] H. T. Langhammer1,T. Muller, T. Walther, R. Bottcher, D. Hesse, E. Pippel, S. G. Ebbinghaus, J Mater Sci (2016) 51:10429-10441; https://doi.org/10.1007/s10853-016-0263-3

[20] Lihong Yang, Hongmei Qiu, Liqing Pan, Zhengang Guo, Mei Xu, Jinhua Yin, Xuedan Zhao, Journal of Magnetism and Magnetic Materials 350 (2014) 1-5; https://doi.org/10.1016/j.jmmm.2013.09.036

[21] Hongxue Liu, Baobao Cao, Charles J. O Connor, Journal of Magnetism and Magnetic Materials 322 (2010) 790-793; https://doi.org/10.1016/j.jmmm.2009.11.004

[22] Chinmay Phadnis, Darshana Y. Inamdar, Igor Dubenko, Arjun Pathak, Naushad Ali, Shailaja Mahamuni, J. Appl. Phys. 110, 114316 (2011); https://doi.org/10.1063/1.3665637